8. N. F. Mott, *Phil. Mag.*, **19**, 835 (1969).
9. G. N. Greaves, *J. Non-Crystalline Solids*, **11**, 427 (1973).
10. V. Ambegaokar, B. I. Halperin, and J. S. Langer, *Phys. Rev. B*, **4**(8), 2612 (1971).
11. M. F. Mataré, *J. Appl. Phys.*, **56**, 2605 (1984).
12. H. R. Zeller, *Phys. Rev. Lett.*, **28**, 1452 (1972).
13. J. W. Orton and M. J. Powell, *Rep. Prog. Phys.*, **43**, 1263 (1980).
14. J. Langer, *Solid State Commun.*, **26**, 839 (1978).
15. M. Jozefowicz, L. T. Yu, J. Perichon, and R. Buvet, *J. Polymer Sci. C*, **22**, 1187 (1969).
16. T. C. Chung, A. Feldblum, A. J. Heeger, and A. G. MacDiarmid, *J. Chem. Phys.*, **74**(10), 5504 (1981).
17. M. Jozefowicz, L. T. Yu, J. Perichon, and R. Buvet, *J. Polymer. Sci. C*, **22**, 1187 (1969).
18. S. Flandrois, *C.R. Acad. Sci. Paris*, **264**, 1244 (1967).
19. M. Salmon, A. F. Diaz, A. J. Logan, M. Krounbi, and J. Bargon, *Mol. Cryst. Liq. Cryst.*, **83**, 265 (1982).

Structure and Activity of Quinolone Antibacterial Agents. 1. 7-Substituted 1-Ethyl-6-fluoro-1,4-dihydro-4-oxoquinoline-3-carboxylic Acids

Youn Ho Shin and Eung K. Ryu

Korea Research Institute of Chemical Technology, P.O. Box 9, Daedeog-Danji, Taejeon 305-606

Young Kee Kang*

Department of Chemistry, Chungbuk National University, Cheongju, Chungbuk 360-763. *Received March 19, 1990*

To find out a correlation between antibacterial activity and physical properties of 7-substituted 1-ethyl-6-fluoro-1,4-dihydro-4-oxoquinoline-3-carboxylic acid, dipole moments, charge distributions, and hydrophobicities were calculated. The atomic charges and the dipole moments to not give any correlations with inhibition of DNA gyrase, but the calculated hydration free energies show some correlations.

Introduction

The quinolone-carboxylic acids as antibacterial agents have been extensively explored for the broad spectrum antibacterial activity and orally effective drugs. Since nalidixic acid, the earlier type of the series of these compounds, was introduced in chemotherapy, there have been many efforts to develop the new powerful antibacterial agents.[1]

In recent years, the quantitative structure-activity relationships (QSAR) associated with the quinolones has been increasingly used in drug design. Typically, the predominant variables which are evaluated for correlation with biological activity are usually physicochemical parameters.[2] And the successful applications of the computer automated structure evaluation (CASE) which utilized molecular features inherent within the chemical structure were recently reported by Klopman *et al.*[3]

To explain a mechanism of inhibition of DNA gyrase by quinolone antibacterial agents, a cooperative quinolone-DNA binding model has been proposed.[4] The essential feature of the model is that bound gyrase induces a specific quinolone binding site in the relaxed DNA substrate in the presence of ATP. The proposed functional domains of quinolone antibacterial agents include hydrogen-bonding domain, drug-drug self-association domain, and drug-enzyme interaction domain.

*To whom correspondence should be addressed.

In this work, we have calculated the physical properties such as dipole moment, charge distribution, and hydrophobicity of quinolone analogues. The calculated dipole moments and the charge distributions were used to find out the characteristics of the hydrogen-bonding domain in the molecules, and hydrophobicities were used to characterize drug-drug self-association domain. The aim of this work is to find out the correlations between biological activity and the calculated data, and to design new drugs.

Methods

The selected parent molecule 1-ethyl-6-fluoro-1,4-dihydro-4-oxoquinoline-3-carboxylic acid and its 7-substituted analogues were studied in this work. Their chemical structures are shown in Figure 1. The initial conformations of the selected quinolones were obtained by building, editing, and minimizing the molecules with Alchemy II.[5] Each conformation was refined with MMPMI,[6] which is an extension of MM2 and MMPI molecular mechanics programs. For each lowest-energy conformation, the atomic charges and the dipole moment were calculated with CNDO/2 (ON) method.[7] The hydration free energy of each group of the molecule was computed using the hydration shell model of Kang *et al.*[8] Especially, the hydration shell parameters of hydration shell radius (R_h) and the free energy density of hydration (Δg_h) for F atom were newly determined from best fitting the calculated free energies of hydration of CHF_3 and CF_4 to experi-

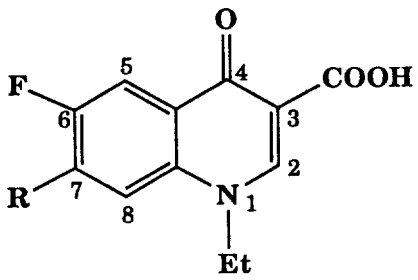

Figure 1. Structure of 7-substituted 1-ethyl-6-fluoro-1,4-dihydro-4-oxoquinoline-3-carboxylic acid; R = H (**1**), chloro (**2**), methyl (**3**), pyrrolidin-1-yl (**4**), piperazin-1-yl (**5**), 1-methylpiperazin-4-yl (**6**), methylamino (**7**), 2-aminoethylthio (**8**), pyrrol-1-yl (**9**), thiazolidin-3-yl (**10**), thiomorpholin-4-yl (**11**).

Table 1. Dipole Moments and Atomic Charges of Some Polar Groups[a]

Compound[b]	Dipole moment (Debye)	Atomic charge (ecu)					
		C[c]	O[c]	C[d]	O[d]	O[e]	H[e]
1	6.58	0.335	-0.349	0.524	-0.376	-0.375	0.219
2	5.62	0.337	-0.347	0.524	-0.374	-0.373	0.218
3	6.82	0.337	-0.354	0.523	-0.377	-0.374	0.219
4	6.69	0.336	-0.356	0.521	-0.379	-0.377	0.220
5	6.98	0.336	-0.358	0.521	-0.376	-0.378	0.220
6	6.74	0.336	-0.357	0.521	-0.377	-0.377	0.219
7	5.85	0.336	-0.356	0.521	-0.377	-0.376	0.218
8	6.73	0.328	-0.339	0.523	-0.339	-0.374	0.218
9	4.86	0.336	-0.352	0.523	-0.372	-0.375	0.219
10	5.32	0.336	-0.357	0.520	-0.375	-0.377	0.220
11	5.12	0.329	-0.342	0.524	-0.342	-0.375	0.219

[a]Calculated results using CNDO/2 (ON) method.[7] [b]The values of inhibition of DNA gyrase are the same as in Table 4. [c]Atoms of 4-keto group. [d]Atoms of keto group of 3-carboxylic acid. [e]Atoms of hydroxy group of 3-carboxylic acid.

mental values, as done before in ref. 8. The Van der Waals radius of *F* atom is 1.47 Å, taken from ref. 9. The obtained values of R_h and Δg_h for *F* atom are 3.26 Å and 8.768×10^{-3} kcal/(mol. Å^3), respectively.

Results and Discussion

The lowest-energy conformations of the molecules **1**–**11** minimised with the MMPMI are found too be similar form each other. Therefore the structures are not drawn and the molecular geometries are not compared with each other in details.

According to the quinolone–DNA binding model,[4] the drug molecules can be assembled inside the single-stranded pocket through hydrogen bonds between the carbonyl groups on the quinolone rings and the hydrogen-bond donors of the DNA bases. From this model, it is possible that the hydrogen bonding affinity has influence on the biological activity of quinolones. The dipole moments and the atomic charges of 3-carboxylic group and 4-keto group were obtained using CNDO/2 (ON) method for comparing hydrogen bonding character by switching the 7-substituents. The calculated dipole moments and charge distributions are represented in Table 1, and a correlation of the dipole moment and biological activity is shown in Figure 2. We could not find any correlation between dipole moments or charge distributions and inhibition of DNA gyrase.[3] This result indicates that the intermolecular hydrogen bondings are not affected largely by the 7-substituents.

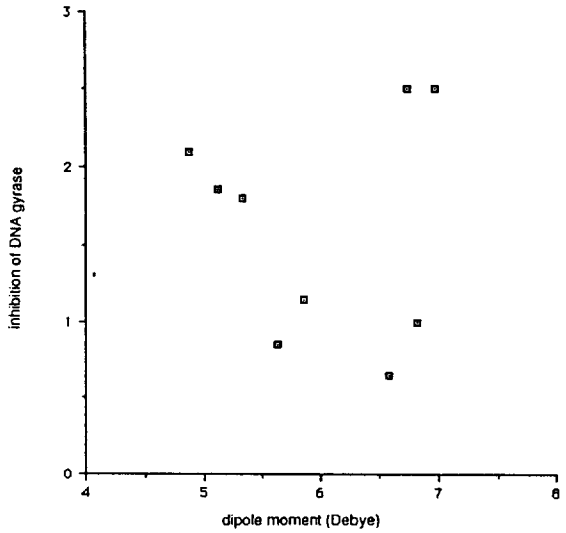

Figure 2. Calculated dipole moments using CNDO/2 (ON) method.

Table 2. Calculated Water-Accessible Volumes and Hydration Free Energies of 6-F Atom[a]

Compound	$V^b_{wa,k}$	$\Delta G^c_{h,k}$	$\Delta G^d_{p,k}$	$\Delta G^e_{hyd,k}$
1	91.8	0.805	0.024	0.829
2	88.5	0.776	0.022	0.798
3	85.1	0.746	0.023	0.769
4	83.5	0.732	0.022	0.754
5	74.7	0.656	0.019	0.675
6	74.6	0.654	0.020	0.674
7	78.4	0.688	0.020	0.708
8	83.4	0.731	0.021	0.752
9	72.3	0.634	0.018	0.652
10	83.4	0.731	0.021	0.752
11	74.6	0.653	0.020	0.673

[a]Calculated using hydration shell model.[8] [b]Water-accessible volumes in Å^3. [c]Hydration free energy coming from water-accessible volume in kcal/mol. [d]Polarization free energy in kcal/mol. [e]Total hydration free energy given by the sum of $\Delta G_{h,k}$ and $\Delta G_{p,k}$ in kcal/mol.

In the quinolone–DNA binding model,[4] the two types of interactions, *i.e.*, the stackings of the quinolone rings and the tail-to-tail hydrophobic interaction between the N-ethyl groups, are proposed. Because of the tail-to-tail interactions between the N1 hydrophobic groups of the quinolone rings are an important feature of the model, we calculated hydrophobicities of N1 atom, 1-ethyl group, and 6-F atom of the molecules using the hydration shell model.

In Tables 2–4, the calculated water-accessibile volume (V_{wa}), hydration free energy ($\Delta G_{h,k}$) coming from V_{wa}, polarization free energy ($\Delta G_{p,k}$) coming from neighboring polar atoms, and total hydration free energy ($\Delta G_{hyd,k}$ where

Table 3. Calculated Water-Accessible Volumes and Hydration Free Energies of N1 Atom[a]

Compound	$V_{wa,k}$	$\Delta G_{h,k}$	$\Delta G_{p,k}$	$\Delta G_{hyd,k}$
1	325.2	-5.038	0.207	-4.831
2	323.8	-5.016	0.201	-4.815
3	322.3	-4.992	0.203	-4.789
4	314.0	-4.863	0.221	-4.642
5	325.1	-5.036	0.229	-4.807
6	325.2	-5.037	0.231	-4.806
7	321.3	-4.977	0.225	-4.752
8	316.8	-4.908	0.225	-4.683
9	320.5	-4.965	0.220	-4.745
10	313.4	-4.854	0.218	-4.636
11	318.4	-4.932	0.235	-4.697

[a]Refer to the footnotes of Table 2.

Table 4. Calculated Water-Accessible Volumes and Hydration Free Energies of 1-Ethyl Group[a]

Compound	$V_{wa,k}$	$\Delta G_{hyd,k}$	Inhibition of DNA gyrase[b]
1	954.3	0.944	0.65
2	951.2	0.942	0.85
3	948.9	0.941	1.00
4	871.6	0.846	—
5	882.0	0.851	2.50
6	883.3	0.853	2.50
7	883.3	0.856	1.15
8	869.5	0.844	—
9	882.7	0.855	2.10
10	870.5	0.845	1.80
11	874.8	0.848	1.85

[a]Refer to the footnotes of Table 2. [b]Experimental data taken from Ref. 3 in μg/ml.

$\Delta G_{hyd,k} = \Delta G_{h,k} + \Delta G_{p,k}$) of the molecules **1-11** are listed. The computed $\Delta G_{hyd,k}$ of the group and atoms and inhibition of DNA gyrase[3] are shown in Figures 3-5.

Figure 3 in which the inhibition of DNA gyrase and the total hydration free energy of 6-F atom are plotted shows somewhat a linear correlation. The inhibitions of DNA gyrase are increased with decreasing the total hydration free energy of 6-F atom. In Figure 4, there was not any relationshiop between the inhibition of DNA gyrase and the total hydration free energy of N1 atom.

In the case of 1-ethyl group, the hydration free energies have an interesting correlation with biological activities, *i.e.*, higher and lower biological activities are associated with the hydration free energies of 1-ethyl group equal to about 0.85 and 0.94 kcal/mol, respectively, as shown in Figure 5. The decrease of hydration free energy of 1-ethyl group is believed to be caused from the water molecules around 1-ethyl group excluded by neighboring groups (see Table 4). As the results, the intermolecular hydrophobic interaction of ethyl-ethyl groups can be increased. This implication is in good agreement with the proposed quinolone-DNA binding model.[4] that the hydrophobic interactions between ethyl groups

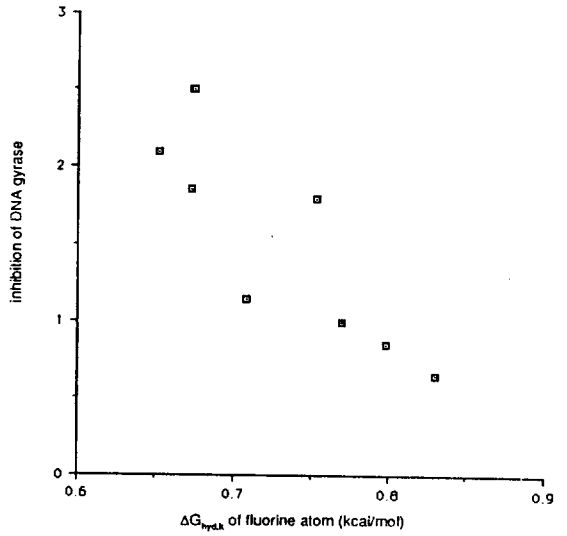

Figure 3. Calculated $\Delta G_{hyd,k}$ of 6-F atom.

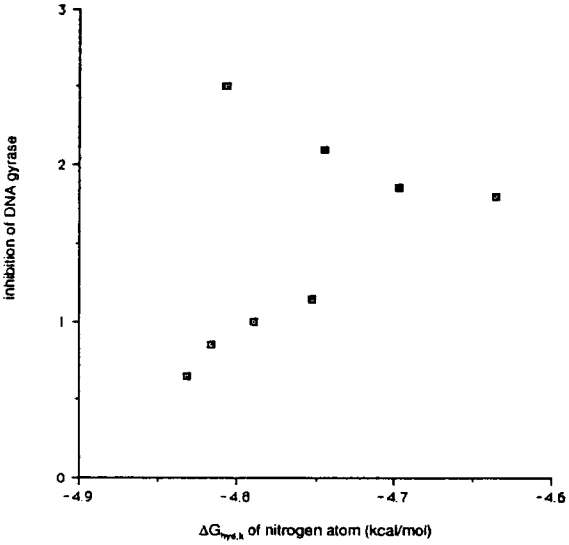

Figure 4. Calculated $\Delta G_{hyd,k}$ of N1 atom.

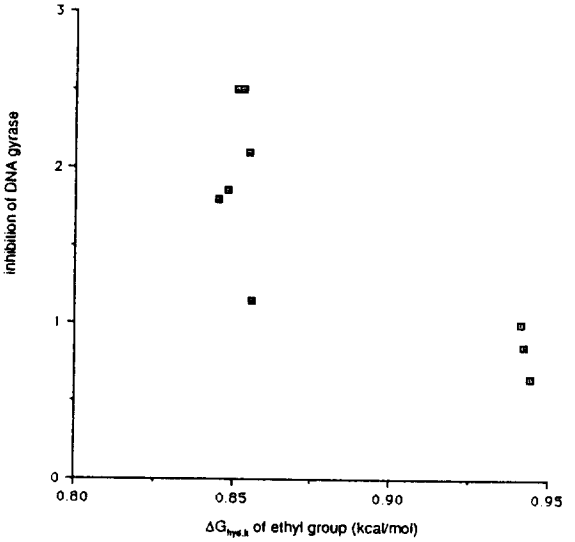

Figure 5. Calculated $\Delta G_{hyd,k}$ of 1-ethyl group.

are the minimum level of interaction needed for the optimal activity even if these interactions are not the sole determinant for the binding affinity.

In conclusion, the hydration free energies calculated using the hydration shell model on some 7-substituted 1-ehtyl-6-fluoro-1,4-dihydro-4-oxoquinoline-3-carboxylic acids show some correlations with their inhibitory activities against DNA gyrase. The calculated dipole moments and charge distributions with CNDO/2 (ON) method do not show any correlations with the activities. The results may serve as a starting step for further studies in understanding the detailed binding affinity and specificity of quinolone analogues with DNA gyrase.

References

1. P. B. Fernandes, *Quinolones*, J. R. Prous Science, Spain, 1989.
2. J. M. Domagala, L. D. Hanna, C. L. Heifetz, M. P. Hutt, T. F. Mich, J. P. Sanchez, and M. Solomon, *J. Med. Chem.*, **29**, 394 (1986).
3. G. Klopman, O. T. Macina, M. E. Levinson, and H. S. Rosenkranz, *Antimicrob. Agents Chemother.*, **31**, 1831 (1987).
4. L. L. Shen, L. A. Mitscher, P. N. Sharma, D. W. T. Chu, C. S. Cooper, T. Rosen, and A. G. Pernet, *Biochemistry*, **28**, 3886 (1989).
5. *Alchemy II*, Tripos Associates, Inc., 1988.
6. N. L. Allinger and Y. H. Yuh, *QCPE* **395**, 1980.
7. J. F. Yan, F. A. Momany, R. Hoffmann, and H. A. Scheraga, *J. Phys. Chem.*, **74**, 420 (1970).
8. Y. K. Kang, K. D. Gibson, G. Nemethyl, and H. A. Scheraga, *J. Phys. Chem.*, **92**, 4739 (1988).
9. A. Bondi, *J. Phys. Chem.*, **68**, 441 (1964).

Preparation, Structure, and Photoemission Studies on the High Temperature Superconductor $YBa_2Cu_{3-x}Ni_xO_{7-\delta}$

Jin-Ho Choy* and Won-Young Choe

Department of Chemistry, Seoul National University, Seoul 151-742. *Received April 9, 1990*

$YBa_2Cu_{3-x}Ni_xO_{7-\delta}$ with x = 0.05, 0.2, 0.4, 0.7 and 1.0 had been prepared by the thermal decomposition of corresponding nitrates. Among them, the sample with x = 0.05 shows above-liquid-N_2 temperature superconductivity with T_c of 88.7K. According to the X-ray diffraction analysis, its crystal symmetry was estimated as orthorhombic with the lattice parameters of a = 3.866Å, b = 3.893Å, c = 11.715Å. The chemical composition of the sample was determined by electron probe microanalysis and the chemical composition around its grain boundaries was carefully studied by the X-ray line scanning technique. From the observed binding energy of Ni-$2p_{3/2}$ orbital electron (B.E. = 853 eV) measured by X-ray photoelectron spectroscopy, the valency state of nickel stabilized in $YBa_2Cu_{2.95}Ni_{0.05}O_{7-\delta}$ oxide lattice could be determined to be Ni(II).

Introduction

$YBa_2Cu_3O_{7-\delta}$ ($0 < \delta < 0.5$) is superconducting[1] above 90 K and has a threefold stacked perovskite structure where the central perovskite unit contains Y while two remaining units contain Ba. Neutron and X-ray diffraction studies[2-5] on the various oxygen contents clearly show that $YBa_2Cu_3O_{7-\delta}$ undergoes an orthorhombic-to-tetragonal phase transition[6,7] at around $\delta = 0.5$ with the drastic diminution of Tc as oxygen disintercalates out of the Cu(1) plane between Ba layers. It becomes now evident that in the $YBa_2Cu_3O_{7-\delta}$ oxide its physical and structural properties depend strongly on its oxygen content and on two dimensional sheets of Cu-O pyramids or one dimemsional chains. Additionally, the influence of other cations in $YBa_2Cu_3O_{7-\delta}$ has been investigated by the perturbation of the perovskite structure through isomorphous substitutions[3,8-12]. The substitution of magnetic rare earth cations for Y clearly shows that the Y site in the lattice has only a minor effect on Tc[3], which suggests the superconductivity developes far from the Y site. However, tremendous decrease in Tc was observed from the substitution of 3d transition metal for Cu[8-12]. Band structure calculations[13] performed on this Y-Ba-Cu-O system also led to the conclusion that the Cu3*d*-O2*p* electrons govern the superconducting properties of this oxide. To understand the mechanism of the superconductivity further on Y-Ba-Cu-O system, it is necessary to study the cation substitution effect for Cu sites along with careful physical characterization. Among the cations substituted, Ni ion is known to occupy preferentially the Cu(2) site in the Y and Ba layers[14] and give only a moderate decrease of T_c[15] as shown in Figure 1. Regardless of enormorous researches on the Ni substitution for Cu, only a few papers[16,17] have discussed on their physical characterizations.

In this paper, we present X-ray diffraction, electron probe microanalysis and X-ray photoelectron spectroscopic studies on $YBa_2Cu_{2.95}Ni_{0.05}O_{7-\delta}$ to estimate the actual site of Ni in the lattice and to gain the information on the role of two different sites of Cu in the lattice through the substitution of Ni ion.

Experimental

Samples of $YBa_2Cu_{3-x}Ni_xO_{7-\delta}$ with x = 0.05, 0.2, 0.4, 0.7,